CHEMISTRY OF MATERIALS
Article

Chem. Mater. **2010,** *22,* 4539–4547 4539
DOI:10.1021/cm100736y

New Prospects in the Conception of IR Electro-Tunable Devices: The Use of Conducting Semi-Interpenetrating Polymer Network Architecture

Pierre Verge,[†] Pierre-Henri Aubert,[†] Frédéric Vidal,[†] Laurent Sauques,[‡] François Tran-Van,[†,§] Sébastien Peralta,[†] Dominique Teyssié,[†] and Claude Chevrot*[,†]

[†]*Laboratoire de Physicochimie des Polymères et des Interfaces* (*EA 2528*), *Structure Fédérative Institut des Matériaux* (*FD 4122*), *Université de Cergy-Pontoise, 5 mail Gay-Lussac, F-95031 Cergy-Pontoise cedex, France, and* [‡]*Délégation Générale de l'Armement CEP* (*LOT*), *16 bis avenue Prieur de la Côte d'Or, F-94114 Arcueil Cedex, France.* [§]*Present address: Laboratoire de Chimie-Physique des Interfaces et des Milieux Réactionnels* (*EA2098*), *Université F. Rabelais, Faculté des Sciences et Techniques, Parc de Grandmont, 37200 Tours, France.*

Received August 12, 2009. Revised Manuscript Received July 1, 2010

A self-supported device with tunable reflective properties in the IR was elaborated from the association of a poly(ethylene oxide) (PEO) network, poly(3,4-ethylenedioxythiophene) (PEDOT), and an ionic liquid, 1-ethyl-3-methylimidazolium bis-(trifluoromethylsulfonyl)imide (EMImTFSI). First, the PEO matrix was optimized as a thin film in order to get a combination of satisfactory mechanical properties (flexibility and stiffness) with high ionic conductivity values in the presence of EMImTFSI. A good balance between mechanical properties and ionic conductivity was obtained for a PEO matrix containing 50% of dangling chains (storage modulus $E' = 8.5$ MPa at room temperature, $T_\alpha = -38$ °C, and $\sigma_{\mathrm{EMImTFSI}} = 1.1$ mS/cm). The chemical polymerization of EDOT within the matrix was carried out at 50 °C under experimental conditions leading to the formation of a PEDOT layer (about 2 μm thick) standing just under the surface of the PEO film, PEO and PEDOT polymers being interpenetrating within this locus in the material. This particular architectural organization was demonstrated through current sensitive atomic force microscopy measurements. Spectroelectrochemistry performed on the IR active layer shows tunable and reversible variations of the reflectivity over the 0.8−25 μm range as a function of the applied voltage between −1.2 and +1.2 V. Interesting contrast values were obtained, namely, $\Delta\%R = 40\%$ at 25 μm. The working capacity of the device does not require an electrical contact running over the entire back of the active layer, a single contact at the very end of the film layer being sufficient.

Introduction

Electrochromic devices (ECDs) have been widely studied in the visible spectral region for applications such as solar control glazing for buildings, windscreens for cars, and optical displays.[1,2] These ECDs require transparent electrodes such as indium tin oxide (ITO) which simultaneously ensure (i) the coating of the electroactive materials, (ii) the transmission of light, and (iii) the current collection. Sandwiched between the two electrodes, an electrolytic medium (common salt or ionic liquid) ensures the ionic conductivity. In ECDs, the electroactive material is commonly a metal oxide (WO_3, NiO, etc.), an organic molecule (viologen), or, more recently, an electronically conducting polymer (ECP).[3−7] This latter class of materials gained popularity due to their ease of processability when adequately substituted, their color range versatility, and short optical transitions delays (or switching times). The optical properties of ECP films from visible through IR range are also known to depend upon their oxidation state. When oxidized, the polaronic and/or bipolaronic states of the ECP strongly absorb in the near-infrared (NIR) region, while upon reduction, they become NIR transparent. When coated on a highly reflective surface such as a gold layer, the ECP reversibly provides the attenuation of the reflectance of the metal electrode. Chandrasekhar et al. proposed electroreflective devices in which the conducting polymer is outward facing, hiding a reflective porous gold layer.[8] In this configuration, the ECP is easily accessible to the ionic species of the electrolyte through the micropores, and the devices operate in reflective mode as seen in Scheme 1A. Similarly inspired configurations were reported by Reynolds et al. with poly(alkylenedioxythiophene) derivatives and by Lemordant et al. with polydiphenylamine as electroactive

*To whom correspondence should be addressed. Tel: (+33)(1) 34257042. Fax: (+33) (1)34257042. E-mail: claude.chevrot@u-cergy.fr.

(1) Rauh, R. D. *Electrochim. Acta* **1999**, *44*, 3165–3176.
(2) Mortimer, R. J. *Chem. Soc. Rev.* **1997**, *26*, 147–156.
(3) Trimble, C; Franke, E.; Hale, J. S.; Woolam, J. A. *Thin Solid Films* **1999**, *617*, 355–356.
(4) Hutchins, M. G.; Butt, N. S.; Topping, A. J.; Gallego, J.; Milne, P.; Jeffrey, D.; Brotherston, I. *Electrochim. Acta* **2001**, *46*, 1983–1988.
(5) Beissière, A.; Marcel, C.; Morcrette, M.; Tarascon, J. M.; Lucas, V.; Viana, B.; Baffier, N. J. *Appl. Phys.* **2002**, *91*, 1589.
(6) Granqvist, C. G. *J. Eur. Ceramic Soc.* **2005**, *25*, 2907–2912.
(7) Beaujugé, P. M.; Reynolds, J. R. *Chem. Rev.* **2010**, *110*(1), 268–320.
(8) Chandrasekhar, P. *Proc. SPIE* **1995**, *2528*, 169.

Published on Web 07/23/2010

Scheme 1. Different Configurations of Electro-Reflective Devices from the Literature[a]

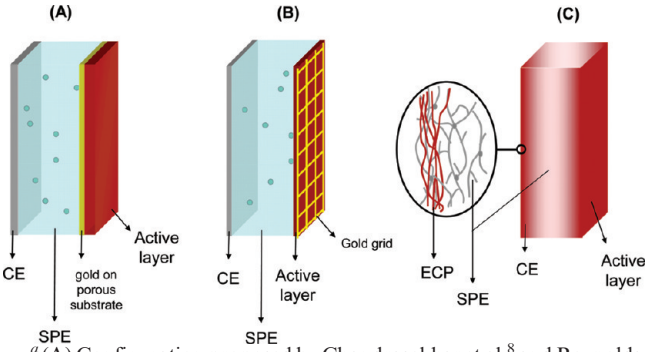

[a] (A) Configuration proposed by Chandrasekhar et al.[8] and Reynolds et al.[12]; (B) configuration proposed by Topart et al.[19]; (C) semi-IPN architecture ECP/SPE/ECP. CE = counter electrode, ECP = electronically conducting polymer, and SPE = supporting polymer electrolyte.

materials for electrochromic displays[9−11] or electroreflective devices.[12−14] Up to 80% of NIR reflective modulation was obtained at 2.0 μm[12] upon application of a low voltage. In all of the above-described systems, the multilayered architecture elaboration remains very complex, hence limiting the commercial development of the devices except in the field of high technology areas (spacecraft, aeronautics, etc.). In all cases, the gold layer component remains essential ensuring current collection as well as highly reflective surface properties, while the ECP ensures modulation of the total reflection upon changes in absorbance. Moreover, ECPs also exhibit variable reflectance properties in the NIR region beyond the plasma frequency as metallic conductors do in the visible range, in the course of the doping/dedoping process. This point was widely investigated in the literature[15−18] through either chemical or electrochemical doping processes of the ECP. Taking into account the reflective properties of ECP, Topart et al. proposed a device in which the polydiphenylamine is deposited on a gold grid,[19] the latter facing outward (Scheme 1B). Nevertheless, this configuration still leads to a multilayered architecture device.

A significant improvement to the multilayered devices stands in the simplification of their architecture, i.e., in reducing as far as possible the number of the necessary building blocks. Mecerreyes et al.[20,21] recently proposed to reduce the number of layers down to five by coating PEDOT films on a solid polymer electrolyte. However, the device operates in transmissive mode, and no reflective properties were reported.

The multilayered architecture can be considerably simplified if, first, a large enough amount of ECP is used such that it becomes a thick and opaque film. The film thus acts both as the current collector and as a tunable reflective layer. A further and final simplification is achieved when the electrolyte and the ECP film are incorporated in a unique hosting matrix. Such a configuration is possible, taking advantage of the semi-interpenetrating polymer network (semi-IPN) concept.[22] This approach was undertaken in our research group for the design of a new type of electrochromic device (see Scheme 1C) made from a poly(ethylene oxide)/poly(3,4-ethylenedioxythiophene) (PEO/PEDOT) semi-IPN.[23] Nevertheless, this pseudo-classical transparent system required ITO electrodes and exclusively worked in the visible range.

In this article, we report the fabrication of an electroreflective device (ERD) working in open air inspired from a similar synthetic pathway. The PEO/PEDOT semi-IPN architecture electroactive material principle is kept although modified and operating with an ionic liquid. Furthermore, it must be stressed that (i) substantially altering the original synthetic pathway described for electrochromic devices [23] leads to an opaque film which can only work as a tunable reflective component, (ii) a gold layer is nolonger required as a basic reflective layer in the system, and (iii) no transparent electrodes are required as current collectors.

The resulting self-supported device exhibits tunable reflective properties and fast optical commutation upon application of a low voltage. Moreover, the device is flexible without any possibilities of delamination of the optical active layers since they belong to an interpenetrating architecture. The modulation of the reflective properties of the device in the IR is studied as a function of the applied voltage. Current sensitive atomic force microscopy (CS-AFM) measurements were performed in order to highlight the relationship between the variation of the dielectric properties and the optical properties of PEDOT. This technique was also helpful to confirm the interpenetration at the microscale level between the PEDOT and the PEO matrix. Finally, switching time, cyclability, and memory effect data of the self-supported device are given as complementary characterizations.

Experimental Section

Chemicals. Polyethyleneglycol dimethacrylate (PEGDM 550 g·mol^{-1}; Aldrich), polyethyleneglycol methacrylate (PEGM 475 g·mol^{-1}; Aldrich), and anhydrous iron(III) chloride $FeCl_3$

(9) Argun, A. A.; Bérard, M.; Aubert, P.-H.; Reynolds, J. R. *Adv. Mater.* **2005**, *17*, 422–426.
(10) Nielsen, C. B.; Angerhofer, A.; Abboud, K. A.; Reynolds, J. R. *J. Am. Chem. Soc.* **2008**, *130*, 9734–9746.
(11) Zhang, J. D.; Yu, H. A.; Wu, X. G.; Wang, Z. Y. *Opt. Mater.* **2004**, *27*, 265–268.
(12) Aubert, P.-H.; Argun, A.; Cirpan, A.; Tanner, D. B.; Reynolds, J. R. *Chem. Mater.* **2004**, *16*, 2386–2393.
(13) Dyer, A. L.; Grenier, C. R.; Reynolds, J. R. *Adv. Funct. Mater.* **2007**, *17*(9), 1480–1486.
(14) Pagès, H.; Topart, P.; Lemordant, D. *Electrochim. Acta* **2001**, *46*, 2137–2143.
(15) Lee, K.; Heeger, A. J. *Synth. Met.* **1997**, *84*, 715–718.
(16) Lee, K.; Reghu, M.; Yuh, E. L.; Sariciftci, N. S.; Heeger, A. J. *Synth. Met.* **1995**, *68*, 287–291.
(17) Chang, Y.; Lee, K.; Kiebooms, R.; Aleshin, A.; Heeger, A. J. *Synth. Met.* **1999**, *105*, 203–206.
(18) Lee, K.; Heeger, A. J.; Cao, Y. *Synth. Met.* **1995**, *72*, 25–34.
(19) Topart, P.; Hourquebie, P. *Thin Solid Films* **1999**, *352*, 234.
(20) Mecerreyes, D.; Marcilla, R.; Ochoteco, E.; Grande, H.; Pomposo, J. A.; Vergaz, R.; Sánchez Pena, J. M. *Electrochim. Acta* **2004**, *49*, 3555–3559.
(21) Pozo-Gonzalo, C.; Mecerreyes, D.; Pomposo, J. A.; Salsamendi, M.; Marcilla, R.; Grande, H.; Vergaz, R.; Barrios, D.; Sanchez-Pena, J. M. *Sol. Energy Mater. Sol. Cells* **2008**, *92*, 101–106.
(22) Klempner, D.; Sperling, L. H.; Utracki L. A. *Interpenetrating Polymer Networks*; Advances in Chemistry Series 239; American Chemical Society: Washington, DC, 1994.
(23) Tran-Van, F.; Beouch, L.; Vidal, F.; Yammine, P.; Teyssié, D.; Chevrot, C. *Electrochim. Acta* **2007**, *53*, 4336–4343.

(Acros) were used as received. EDOT (Bayer) was distilled under reduced pressure at 130 °C. 2,2-Azobisisobutyronitrile (AIBN, Aldrich), was recrystallized from methanol and dried under vacuum prior to use. Methanol (Acros 99.5%) and chloroform (VWR, 99−99.6%) were used without further purification.

Synthesis of Materials. Poly(ethylene oxide)/poly(3,4-ethylenedioxythiophene) semi-IPN was prepared according to the published procedure with the following modifications.[23,24] PEO networks with a given amount of PEO dangling chains are prepared as follows: 0.5 g of PEGM, 0.5 g of PEGDM, 1 wt % AIBN radical initiator, and 50 mg of EDOT are stirred together under argon atmosphere at room temperature. The mixture is poured into a mold made from two glass plates clamped together and sealed with a 500 μm thick Teflon gaskets. The mold is then held at 50 °C for 4 h, and then postcured for 1 h at 80 °C. Finally after cooling at room temperature on glass plates and after Teflon removal, a free-standing EDOT-swollen PEO network is obtained. In order to determine the efficiency of cross-linking reactions, PEO network samples synthesized separately without EDOT are Soxhlet extracted: the extracted amount of nonreacted PEGM or PEGDM starting material is less than 1 wt % for all synthesis. The EDOT-swollen PEO films are immersed in a $FeCl_3$ saturated chloroform solution in order to promote the oxidative polymerization of EDOT. The time and temperature conditions are adjusted until a homogeneous dark blue coloration is obtained. Sulfur elemental analyses are performed on all samples allowing the determination of the PEDOT content. At 25 °C, the PEDOT content increases from 0.3 to 1.1 wt % as a function of polymerization time from 1 to 24 h, whereas at 50 °C the PEDOT content varies from 1.1 to 4.9 wt % for the same variation in polymerization time. The film is washed three times with methanol to remove the excess $FeCl_3$ and unreacted EDOT. All PEO/PEDOT semi-IPNs discussed hereafter have been prepared according to this procedure.

The synthesis of room temperature ionic liquid, 1-ethyl-3-methylimidazolium bis-(trifluoromethylsulfonyl)imide (EMImTFSI), was carried out according to the procedure described by Grätzel et al.[25]

Measurements. The measurements for the determination of the diffusion coefficients of EDOT from the PEO networks to $CHCl_3$ ($D_{EDOT\rightarrow CHCl3}$), i.e., during the swelling in $FeCl_3$ solution EDOT swollen PEO networks, prepared as previously described, have been dipped in $CHCl_3$ for different lengths of time at 20 °C. The amount of EDOT diffused in $CHCl_3$ has been characterized from the Beer−Lambert law measuring its absorbance at 248 nm. The value of $D_{EDOT\rightarrow CHCl3}$ has been calculated from the second Fick diffusion law. The same experiment has been performed at −2, 15, and 30 °C to calculate the Arrhenius law parameters in order to determine the value of $D_{EDOT\rightarrow CHCl3}$ at 50 °C. For the $FeCl_3$ diffusion coefficient, PEO networks have been dipped in a 0.23 mol·L^{-1} $FeCl_3/CHCl_3$ solution for different lengths of time. The networks have been removed and washed in methanol. The $FeCl_3$ contents in the networks have been determined from the Beer−Lambert law measuring its absorbance at 365 nm in methanol. The diffusion coefficient of $FeCl_3$ in the PEO networks has been calculated considering that the diffusion of the ferric species within the network follows the second Fick diffusion law.

The NIR optical characterizations were performed in reflectance mode using an integrated sphere (60 mm diameter) mounted onto a JASCO V-570 spectrophotometer. The scan rate was set to 1000 nm/min between 800 nm and 2500 nm. IR characterizations were performed from 2.5 to 25 μm using a Fourier Transform Infra-Red spectrophotometer (Nicolet-Magnar IR) fitted to a hemispheric reflectometer SOC 100 extension. Current-sensing mode AFM (CS-AFM) imaging was performed on a Dimension D3100 (Veeco) controlled by Nanoscope IIIa software and a Tuna extension module (Veeco). The CS-AFM images were acquired in open air with the contact mode using a conducting probe (ElectriCont by BudgetSensor, Cr/Pt coated, spring constant 0.2 N/m, resonant frequency 13 kHz). The load force was maintained at 2−6 nN to avoid damaging the sample. A +1 V voltage was applied between the tip and the sample, the latter being connected to the ground. When the sample was too insulating, the voltage was increased up to +5 V in order to increase the current contrast. It is then possible to record simultaneously the topography and the current distribution. Such a procedure does not imply any doping or oxidation level change of the PEDOT since the images are reproducible. For the study, the surface of the cross-section was prepared by cryo-ultramicrotomy (Leica Ultracut UCT) using a 35° diamond knife. Dynamic mechanical analysis (DMA) measurements were carried out on samples (typical $L \times w \times t = 15 \times 8 \times 0.5$ (mm)) with a Q800 model (TA Instruments) operating in tension mode (strain between 0.05 and 0.07%; pretension, 10^{-2} N). Experiments were performed at 1 Hz frequency and with a heating rate of 3 °C/min from −100 to +50 °C. The setup provided the storage and loss moduli (E' and E''), and the damping parameter or loss factor (tan δ) was defined as $\tan\delta = E''/E'$.

Results and Discussion

1. Synthesis and Characterizations of the PEO/PEDOT Semi-IPN. Synthesizing the PEO based host matrix is the key point in order to manage a film material with both high conductivity when swollen with EMImTFSI and low tear ability, keeping in mind that all PEO compositions here will be in a rubbery state at 25 °C. The PEO branched network is obtained by free radical copolymerization of PEGDM and monofunctional PEGM with AIBN as initiator (1 wt % with respect to total methacrylic functions). High levels of cross-linking density, i.e., increasing the PEGDM content will serve the low tear ability purpose. However, the concomitant resultant decrease in the amount of dangling PEGM chains will decrease the available free volume for ion mobility.[26] The two terms are contradictory, but a satisfactory compromise was obtained screening three compositions containing 25, 50, and 75 wt % PEGM. This preliminary study has been performed in the absence of the EDOT reactant.

The viscoelastic behavior of EDOT free PEO networks was studied by DMA and both the E' modulus at 25 °C and the α-relaxation temperatures (T_α) are presented in Table 1. As expected, E' increases with the PEGDM (cross-linker) content. In the same manner, T_α increases from −47 °C to −30 °C with the cross-linking density with PEGDM contents increasing from 25% to 75%. It should be pointed out that the less cross-linked material (PEGM/PEGDM 75/25) can hardly be handled because of the

(24) Verge, P.; Vidal, F.; Aubert, P.-H.; Beouch, L.; Tran-Van., F.; Goubard, F.; Teyssié, D.; Chevrot, C. *Eur. Pol. J.* **2008**, *44*, 3864–3870.
(25) Bonhôte, P.; Dias, A.-P.; Papageorgiou, N.; Kalyanasundaram, K.; Grätzel, M. *Inorg. Chem.* **1996**, *35*, 1168–1178.
(26) Plesse, C.; Vidal, F.; Randriamahazaka, H.; Teyssié, D.; Chevrot, C. *Polymer* **2005**, *46*, 7771–7778.

Table 1. Mechanical, Swelling, and Ionic Conductivity Properties of the PEO Networks Obtained According to the PEGM/PEGDM Ratio Used during the Polymerization

PEGM/PEGDM ratio	25/75	50/50	75/25
storage modulus E' (MPa)	16.5	8.5	6
T_α (°C)	−30	−38	−47
EMImTFSI swelling ration (% wt)	100	138	320
ionic conductivity (mS/cm) at 30 °C	0.3	1.1	1.7

very weak tear resistance. Table 1 shows also the EMImTFSI uptakes for PEO networks at their maximum swelling capacities. As far as the cross-linking density of the PEO phase is concerned, the EMImTFSI uptake decreases from 320 to 100 wt % when the relative weight proportion of PEGDM increases from 25 to 75 wt %. Ionic conductivity measurements performed on EMImTFSI-saturated networks show that the higher ionic conductivity is obtained for PEO networks containing 25 and 50 wt % PEGDM and reaches the same order of magnitude, i.e., 10^{-3} S·cm^{-1} even for different EMImTFSI contents according to the PEGM/PEGDM ratio. For 75 wt % PEGDM, the ionic conductivity decreases to 0.3×10^{-3} S·cm^{-1} as a consequence of both the low content of dangling chains and the low EMImTFSI uptake. Finally and in the following, only PEO networks with an equivalent PEGM/PEGDM proportion (50/50 in weight) were used as hosting matrix for the electroreflective device. Indeed, only such a material displays both a good tear resistance and a high ionic conductivity when swollen with EMImTFSI.

PEO/PEDOT semi-IPNs were then prepared. Whereas the phase domain size in full IPNs lies between 50 and 500 nm as a general observation ensuring a high homogeneity and even sometimes a synergy in the properties, the phase domain size in the case of semi-IPNs usually lies in the 500 nm−3 μm range.[27] The semi-IPN phase domain size sometimes is of the same order of magnitude as what can be observed in composites or blends; however, the consequences (flow and creep) of this phase separation in semi-IPNs are not the same as those in blends and can be overcome by thermodynamical parameters and/or suitable chemical affinity between the two partner compounds. In this respect, the affinity of ethylenedioxythiophene segments in PEDOT for ethylenedioxy units in PEO could be an asset. Thus (PEO/PEDOT), semi-IPNs were prepared by dipping the EDOT (5 wt %) swollen PEO network films into a $FeCl_3$ saturated chloroform solution for 1 h at 50 °C. PEDOT is thus obtained in its doped state. These experimental conditions were chosen because the best contrast value in reflection in the IR was obtained (vide infra). This synthesis pathway leads to a PEDOT content of 1.1 wt % with an anisotropic repartition throughout the thickness of the film: indeed, PEDOT is located in equivalent amounts on each edge, i.e., on the two sides, of the semi-IPN. Different processes govern the symmetrical and anisotropic distribution of the electronic conducting polymer throughout the thickness of the PEO networks. Among these processes, the diffusion of EDOT from the film to the chloroform solution and the diffusion of $FeCl_3$ into the matrix play a major role. Since the apparent diffusion coefficient of the EDOT monomer in $CHCl_3$ ($D_{EDOT} = 1.4 \times 10^{-4}$ cm^2/s at 50 °C) is 2 orders of magnitude higher than the diffusion of $FeCl_3$ into the matrix ($D_{FeCl3} = 1.0 \times 10^{-6}$ cm^2/s at 50 °C), the nucleation process for PEDOT growth occurs underneath the film surface. The final amount of PEDOT can easily be controlled through the polymerization reaction time. One way to bring out the repartition of PEDOT in the conducting semi-IPN is to record the electrical response at the micrometer level using an AFM imaging technique, running in current-sensitive mode (CS-AFM).[28,29] The resolution of CS-AFM is as small as the tip−sample contact area, which can be less than 20 nm. Nowadays, its potential for the study of electrical properties of organic semiconductors has been established such as I−V characteristics of oligothiophene,[30] hole transport properties in MEH−PPV,[31] or electrodeposited PEDOT[32] or polypyrrole.[33] This technique was helpful in the case of semi-IPN to characterize both their cross-section and their surface, giving new insights about the inhomogeneous but symmetrical repartition of PEDOT throughout the thickness of the semi-IPN.

According to the procedure described in the Experimental Section, measurement of the electrical current distribution over the cross-section of the freshly synthesized semi-IPN is depicted in Figure 1A. The left part of the image corresponds to the central part of the semi-IPN film, while the right side matches the outer part (edge or surface) of the semi-IPN. On the left, a continuous near zero current reveals an insulating phase corresponding to a rich PEO domain (brown color). Moving toward the edge, i.e., the right part of the picture, the current level is increasing (lighter color). This means that doped PEDOT, consistent with the chemical oxidative synthesis, is present in this locus in the form of an interpenetrating PEO/PEDOT phase. From this observation, the penetration's depth of PEDOT can be estimated as 2 μm (Figure 1A). In comparison with the energy-dispersive X-ray spectroscopy (EDX) measurements carried out on similar architectures,[34] the analogy between the current increase and the presence of PEDOT near the surface is clear. It is important to note that comparable current topologies are observed at the other edge of the sample and whatever the cross-section confirming the fact that the PEDOT amounts on the two surface regions of the film are similar. All this indicates that the penetration depth of the PEDOT is constant on each surface.

(27) Donatelli, A. A.; Sperling, L. H.; Thomas, D. A. *Macromolecules* **1976**, *9*, 671–676.
(28) Shafai, C.; Thomson, D. J.; Simard-Normandin, M.; Mattiussi, G.; Scanlon, P. J. *Appl. Phys. Lett.* **1994**, *64*, 342.
(29) De Wolf, P.; Snauwaert, J.; Clarysse, T.; Vandervorst, W.; Hellemans, L. *Appl. Phys. Lett.* **1995**, *66*, 1530.
(30) Kelley, T. W.; Frisbie, C. D. *J. Vac. Sci. Technol. B* **2002**, *18*, 632.
(31) Lin, H. N.; Lin, H. L.; Wang, S. S.; Yu, L. S.; Perng, G. Y.; Chen, S. A.; Chen, S. H. *Appl. Phys. Lett.* **2002**, *81*, 2572.
(32) Han, D. H.; Kim, J.-W.; Park, S. M. *J. Phys. Chem. B* **2006**, *110*, 14874–14880.
(33) Lee, H. J.; Park, S. M. *J. Phys. Chem. B* **2004**, *108*, 1590–1595.
(34) Vidal, F.; Popp, J. F.; Plesse, C.; Chevrot, C.; Teyssie, D. J. *Appl. Polym. Sci.* **2003**, *90*, 3569–3577.

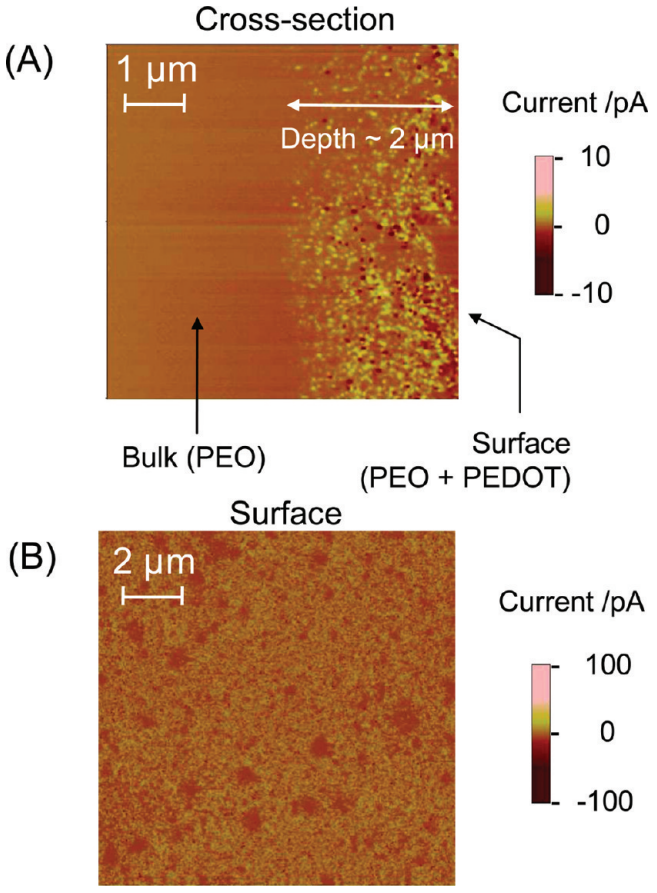

Figure 1. (A) CS-AFM picture of the cross-section of the semi-IPN PEO/PEDOT. (B) CS-AFM picture at the surface of the semi-IPN freshly synthesized.

Figure 1A also indicates that the submicrometer range phase separation is consistent with a typical semi-IPN architecture as highlighted by the current topology. This limited PEO/PEDOT phase separation level due to favorable interactions between the two polymers does not preclude the development of interesting electro-active properties.

Figure 1B shows the surface of the same semi-IPN using again the current sensitive mode of the AFM. The apparent current level is about 30−40 pA, indicating that all of the PEDOT is in its doped form. The repartition of PEDOT is rather uniform at this scale, whatever the area probed by the tip as Park et al.[32,33] reported with electrodeposited PEDOT. Finally, attention can be drawn to some small domains which appear more insulating (browner spots, with a diameter of ~1 μm) as a consequence of a PEO/PEDOT phase containing either more PEO or PEDOT in its neutral form.

The insulating-to-conducting transition induced by a chemical doping/dedoping process of the surface located PEDOT in the semi-IPN was also characterized through CS-AFM mode. Figure 2 shows a 10 μm × 10 μm mapping of the current distribution at the surface of a PEO/PEDOT chemically reduced by immersing the PEO/PEDOT semi-IPN in an aqueous hydrazine solution (Figure 2A,B) and the subsequently PEO/PEDOT chemically oxidized by immersion in an aqueous $NOBF_4$ solution (Figure 2C).

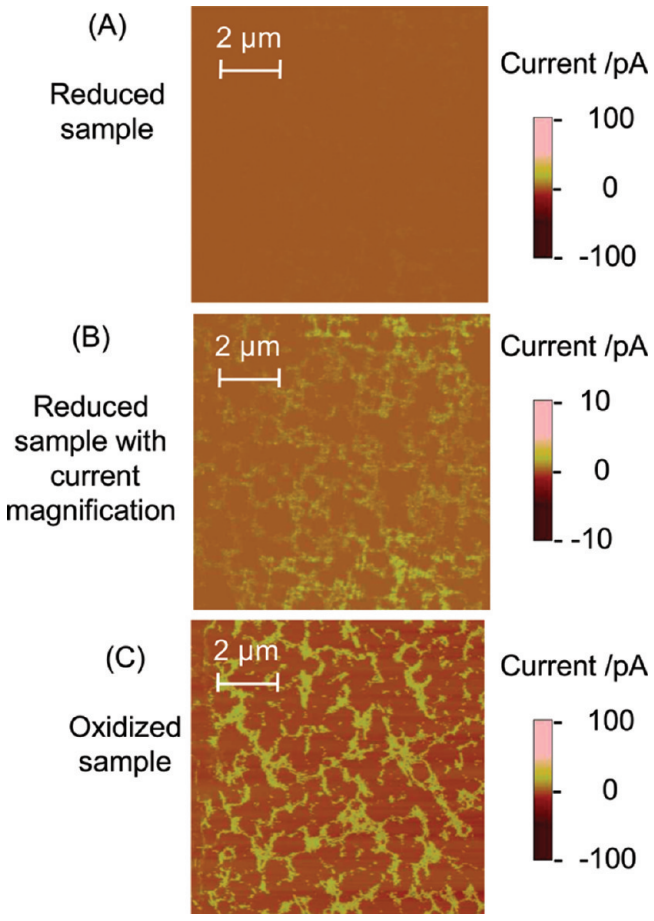

Figure 2. CS-AFM pictures of the active layer of a PEO/PEDOT semi-IPN (A) reduced by immersion in an aqueous hydrazine solution; (B) the same region of film as that in A but with higher current sensivity; (C) chemically oxidized by immersion in an aqueous $NOBF_4$ solution.

Figure 2A reveals the homogeneous current's levels near 0 pA with a low electronic conductivity in the full current scale (0−100 pA) due to the PEDOT dedoping process by hydrazine. However, focusing on the current level, it is possible to improve the contrast by applying additional voltage (ΔV = 5 V). Indeed when decreasing the scale sensitivity at 10pA, a slight contrast appears (see Figure 2B). As these experiments were performed in open air conditions, this residual low conductivity can be assigned to the reoxidation of the dedoped form of PEDOT by oxygen.[35,36]

Upon oxidation of PEDOT with $NOBF_4$, the current level increases leading to a better contrast (Figure 2C). Surprisingly, the insulating regions appear larger in comparison to the conducting ones. Possible explanations could be suggested: (i) some overoxidation processes of the PEDOT could occur, leading to a poorer charge carrier density as suggested by Bredas et al., and [37] (ii) the morphology and roughness of the film is changing according to the doping level given that the redox processes lead to a volume change in the case of ECPs.

(35) Johansson, T.; Pettersson, L. A. A.; Inganäs, O. *Synth. Met.* **2002**, *129*, 269–274.
(36) Chun-Guey, W.; Mei-Jui, C.; Yii-Chung, L. *J. Mater. Chem.* **1998**, *8*, 2657–2661.
(37) Bredas, J. L.; Elsenbaumer, R. L.; Chance, R. R.; Silbey, R. J. *J. Chem. Phys.* **1983**, *78*, 5656.

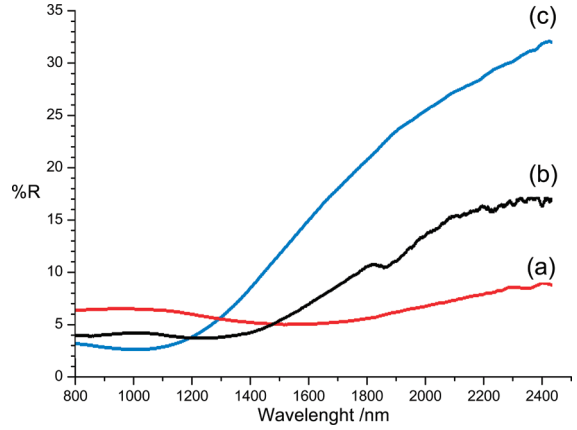

Figure 3. Reflectance spectra from 0.8 to 2.5 μm in the NIR of the active layer of a PEO/PEDOT semi-IPN reduced by immersion in an aqueous hydrazine solution (curve a), freshly synthesized (curve b), and oxidized by immersion in an aqueous $NOBF_4$ solution (curve c).

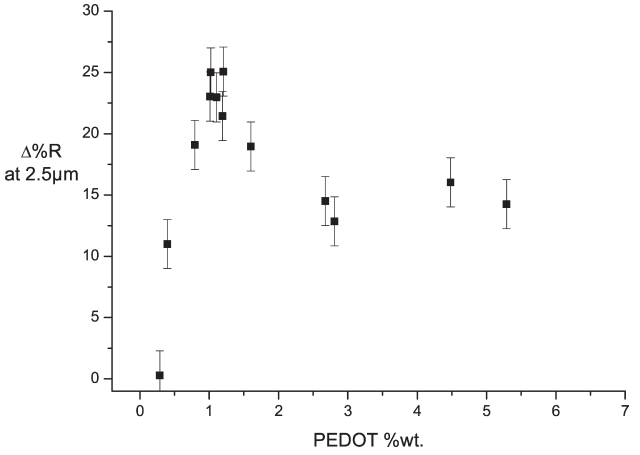

Figure 4. Evolution of the contrast reflectance at 2.5 μm ($\Delta\%R_{2.5\,\mu m}$) as a function of the PEDOT content (%wt) in the semi-IPN. $\Delta\%R_{2.5\,\mu m}$ is measured as the difference of the reflectance levels at 2.5 μm between the oxidized and reduced states $(\%R_{ox} - \%R_{red})_{2.5\,\mu m}$.

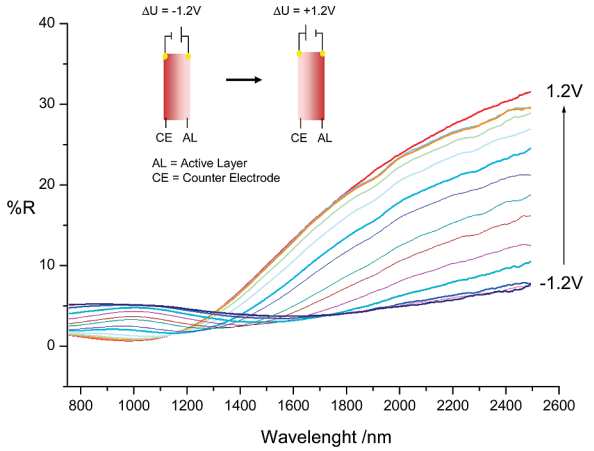

Figure 5. Spectroelectrochemistry from 0.8 to 2.5 μm in the NIR of a PEO/PEDOT device for applied voltages on the active layer from −1.2 V to 1.2 V recorded every 200 mV step potential. The PEDOT content is 1.1 wt %, and the device was swollen by EMImTFSI (8 wt %).

The reflectance spectra in the 0.8−2.5 μm NIR range for the neutral, freshly synthesized and fully oxidized surfaces studied by CS-AFM are reported in Figure 3. As the variation of conductivity and the NIR modulation of reflectance depend on the doping level of the PEDOT, Figures 1B, 2A, 2C, and 3 allow drawing a correlation between the observed changes. In the NIR spectrum of the reduced semi-IPN (Figure 3, curve a) the reflectance value at 2.5 μm ($\%R_{2.5\,\mu m}$) reaches about 7%, which is in accordance with the weak surface conductivity observed in Figure 2A. The most oxidized PEDOT (Figure 3, curve c) gives the highest reflective response, $\%R_{2.5\,\mu m}$ attaining 33%. This case also corresponds to the most numerous conducting PEDOT areas (Figure 2C). Finally, the freshly synthesized semi-IPN possesses an intermediate oxidation state due to the fact that PEDOT is not fully oxidized during the polymerization process: in this case, $\%R_{2.5\,\mu m}$ is about 16% (Figure 3, curve b) in agreement with the intermediate doped level of PEDOT shown in Figure 1B. From these results, it is noteworthy that not only a good correlation exits between the conductivity and reflectivity changes of PEDOT but also the modulation of the oxidation state of the ECP at the semi-IPN surface leads to potentially tunable optical reflective properties of the active layer in the NIR range. These features represent an illustration of the insulating-metal transition, a well-known phenomenon in the field of conducting polymers and widely described by Heeger.[15] This transition is further evidenced by spectroelectrochemical characterizations presented hereunder.

After PEO/PEDOT semi-IPNs were swollen with an ionic liquid (IL) EMImTFSI, the spectroelectrochemical reflective behavior in the NIR was carried out. As PEDOT is symmetrically distributed on each side of the network film, the semi-IPN is similar to an electrochemical cell with a battery-like configuration, where the inner EMImTFSI PEO swollen network ensures the ionic conductivity, while the comparatively outer PEDOT acts as an electrode. Clearly, the significant interest of such one-piece devices is to operate without any need of ITO electrodes or a gold layer. Moreover, one of the PEDOT layers acts as the current collector as well as an active reflective surface with tunable properties; the other PEDOT layer acts as the counter-electrode. First, a set of PEO/PEDOT semi-IPNs have been prepared in which the PEDOT content is increased by increasing the polymerization time. For each PEDOT content, the reflectance of 8 wt % EMImTFSI swollen semi-IPNs was measured by applying a voltage of +1.2 V (most oxidized PEDOT) and after −1.2 V (most reduced PEDOT), leading to more reflective and less reflective PEDOT, respectively. The difference between the two states represents the optical contrast $\Delta\%R$ at 2.5 μm. Figure 4 clearly indicates that the reflectance contrast is optimized for PEDOT content around 1.1% (corresponding to 1 h oxidative polymerization time). In the following discussion, all semi-IPN samples are studied with this optimized PEDOT content

2. Spectroelectrochemical Characterizations of the Device in Infrared. The controlled modification of the optical reflectance of the active surface in the IR was then studied as a function of the applied voltage. First, Figure 5 shows the spectroelectrochemical behavior of the active layer

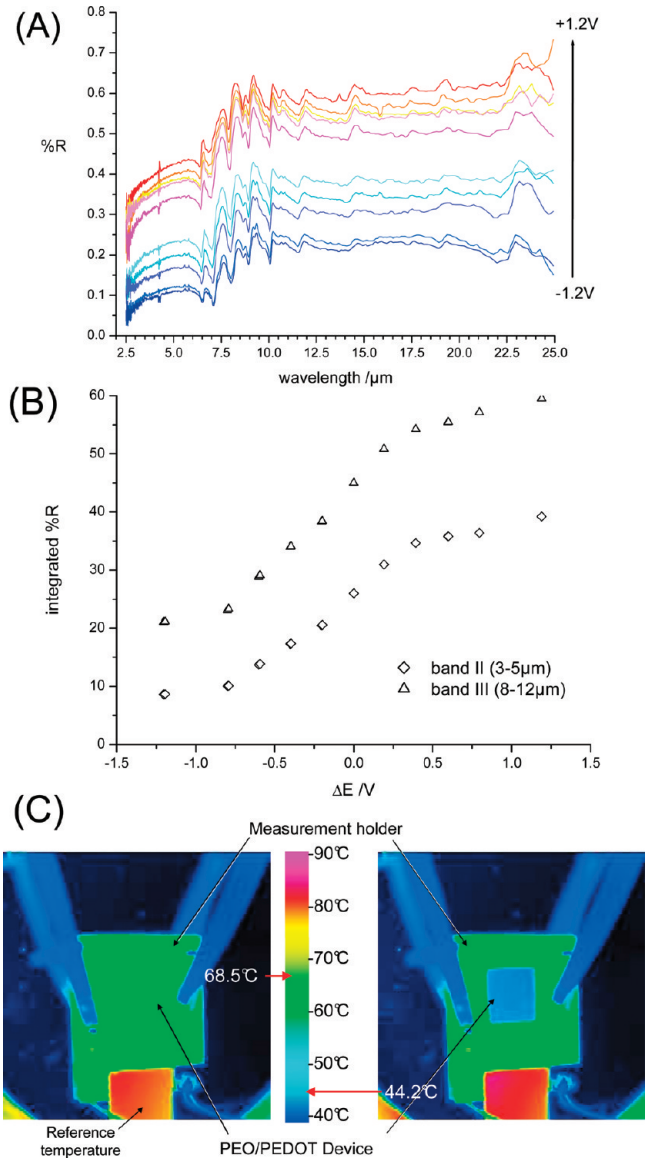

Figure 6. (A) Spectroelectrochemistry from 2.5 to 25 μm in IR of a PEO/PEDOT device for applied voltages on the active layer from −1.2 V to 1.2 V recorded every 200 mV step potential. (B) Integrated reflectance in characteristic band II (3−5 μm) or band III (8−12 μm) regions. (C) IR picture of the device recorded in band III at 70 °C showing apparent temperature according to the doping level of the active layer, 68.5 or 44.2 °C, when reduced or oxidized, respectively. EMITFSI content: 8 wt %.

in the NIR range for voltages with 200 mV steps from −1.2 V to +1.2 V corresponding, respectively, to the most reduced and the most oxidized states of the PEDOT in the semi-IPN. The tuneability of the optical properties of the active layer is demonstrated, leading to a maximum contrast $\Delta\%R$ of 25% at 2.5 μm, which is a very promising behavior in the NIR.

Second, looking at higher wavelengths, Figure 6A shows the spectroelectrochemical behavior of the semi-IPN demonstrating as well the tuneability in the middle IR (between 2.5 and 25 μm) as a function of the applied voltage. The reflectance $\%R$ varies from about 10% to 40% between 2.5 and 7.5 μm for an applied voltage varying from −1.2 V to +1.2 V. Then, the reflectance contrast appears lower than the 60% of contrast reported by Schwendeman et al.[38] between 2 and 5 μm for a multilayer device type A (see Scheme 1). However, in the 10 to 25 μm range, the $\%R$ varies from 20 to 60% for the same applied voltage variation. Although again slightly lower than reported values in the literature,[8,14,19,39] it must be stressed that these data have been obtained without a reflective gold layer as in multilayer devices. Values extracted from Figure 6A are reported in Figure 6B, representing the evolution of the integrated reflectance level as a function of the applied voltage in bands II (3−5 μm) and III (8−12 μm), which are typical IR camera bandwidth. The integrated reflectance contrasts are 30% and 37% in band II and band III, respectively.

These reflectance contrasts can be visualized using an IR camera as shown in Figure 6C. Indeed, the IR camera allows one to show the temperature distribution over a large area of a target surface in a single image.[39] This technique covers a broad domain of applications such as hot spot detection (fire care) as well as energy control (buildings, spacecrafts, etc.). The IR camera measures the radiance of the target surface. After calibration with a blackbody, this radiance can be linked to an apparent temperature. The radiance of an opaque material is dependent on its temperature and on its reflectivity (or emissivity). Figure 6C shows the thermal images of an experiment carried out on the device at thermal equilibrium ($T_{eq.}$ = 70 °C) with a camera operating in the 8−12 μm range (band III). When the active layer was held in the reduced state, the device is hardly noticeable since in these experimental conditions, the support and the device have almost identical radiance (Figure 6C, left image). The apparent temperature is close to equilibrium temperature (68.5 °C). By applying a voltage of +1.2 V, the oxidation of the active layer leads to a modification of its reflectivity, which in turn modifies the apparent temperature (Figure 6C, right image). The active layer of the device appears at a lower temperature (44.2 °C), demonstrating that the device can also be used for IR furtivity purposes.

These results clearly demonstrate that the modulation of the optical properties is reached by the control of the oxidation state of the ECP. Thus, such a device acts on its own as an adaptative optical material, meaning that a desired $\%R$ value can be finely tuned according to the PEDOT doping state through the applied voltage.

3. Switching Time, Cyclability, and Memory Effect of the Device. Switching times of the device at ambient temperature were determined by monitoring the contrast variation at 2.5 μm as a function of time for the doping−dedoping processes of PEDOT in the semi-IPN (Figure 7). In this case, the EMImTFSI content is 8 wt %. As shown in Figure 7, commutation toward the full reduced (dedoped) state is slower (2 min 45 s) than the reversed switch (47 s),

(38) Schwendeman, I; Hwang, J; Welsh, D. M.; Tanner, D. B.; Reynolds, J. R. *Adv. Mater.* **2001**, *13*(9), 634–637.

(39) Madding, R. P. *Emissivity Measurement and Temperature Correction Accuracy Considerations*; Thermosense XXI: Proceedings of SPIE; The International Society for Optical Engineering: Orlando, FL, 1999; Vol. *3700*; pp 393−401.

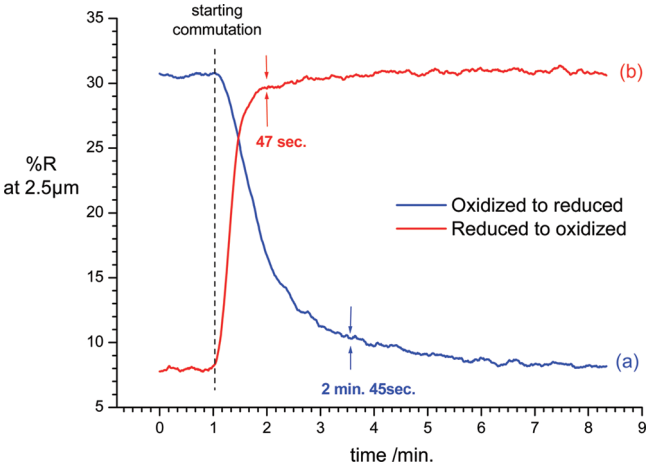

Figure 7. Variation of the reflectance at 2.5 μm (%$R_{2.5\ \mu m}$) during one commutation as a function of time from the oxidized to the reduced state (blue curve) or from the reduced to the oxidized state (red curve) of the PEDOT active layer. The PEDOT content is 1.1 wt %, and the device was swollen by 8 wt % EMImTFSI.

which can both be considered as satisfactory values taking into account the fact that the PEDOT active layer is the one and only current collector. Moreover, the commutation toward the reduced state is expectedly slower since the PEDOT becomes insulating during the process. This arises from the electrical percolation process as has already been reported.[40,41]

Figure 8A shows the evolution of the switching time as a function of EMImTFSI content at room temperature. Also for the reflective/absorbent and absorbent/reflective transitions, an EMImTFSI weight content higher than 10% leads to the lowest switching time (probably because the ionic conductivity level reaches its upper value). Next, the evolution of the switching time as a function of the temperature for 20 wt % EMImTFSI (Figure 8B) was carried out. Increasing the temperature, we observed that the contrast response time drops as expected from 22 s at 28 °C to 6 s at 50 °C, and only 3 s at 80 °C.

The electrochemical cyclability of the device has been examined for 20 wt % EMImTFSI as a function of cycles at 3 working temperatures (25, 60, and 100 °C) in open air (cf. Figure 9). The device was switched between −1.2 V and +1.2 V every 2 min and the electrochemical charge Q_n (C) was recorded for each nth cycle. At ambient temperature, no electroacitivty loss is observed during the first 5 000 cycles. After 20 000 cycles, 80% of relative electroactivity was still remaining, which is very satisfactory for a device operating in open air. Increasing the temperature to 60 °C, we observed that the electroactivity follows the same trend until the 5 000th cycle compared to that in the experiment at 25 °C. Then, the loss is more pronounced and drops rapidly after 10 000 cycles. At 100 °C, the electroactivity cannot be maintained more than 1 000 cycles, and the complete loss of electroactivity occurs before 3 000 cycles. These results can be related to the fact that

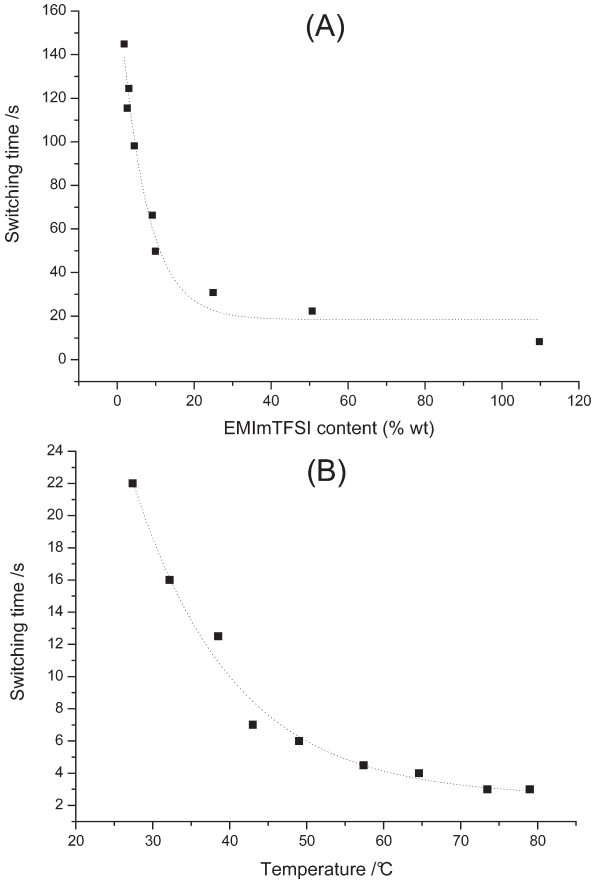

Figure 8. (A) Evolution of the switching time of the PEO/PEDOT device from the reduced to the oxidized state as a function of EMImTFSI weight content at optimized PEDOT content (1.1 wt %). (B) Evolution of the switching time of the PEO/PEDOT device from the reduced to the oxidized state as a function of temperature at 1.1 wt % PEDOT and 20 wt % EMImTFSI.

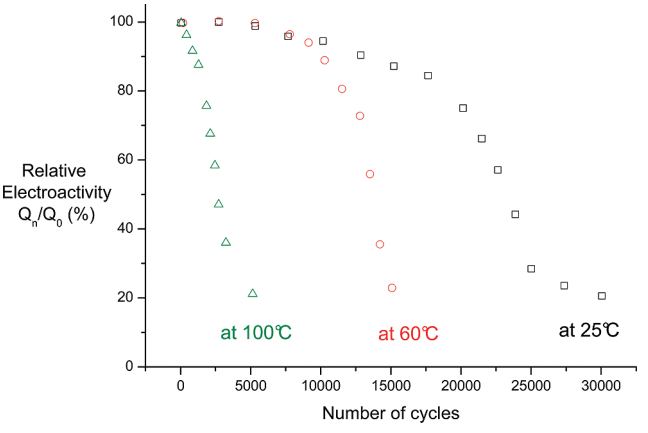

Figure 9. Relative electroavivity of the device Q_n/Q_o (%) recorded during repetitive electrochemical commutations of the device every 2 min between −1.2 V and +1.2 V. The experiment was performed at 25 °C (□), 60 °C (○), and 100 °C (△) in open air, using EMImTFSI (20 wt %) as the electrolyte.

we have shown that PEO/PEDOT semi-IPN exhibit thermal aging in open air conditions:[42] the PEO network

(40) Aoki, K.; Cao, J.; Hoshino, Y. *Electrochim. Acta* **1994**, *39*(15), 2291–2297.
(41) Aoki, K. *J. Electroanal. Chem.* **1994**, *373*, 67–73.
(42) Verge, P.; Vidal, F.; Aubert, P.-H.; Beouch, L.; Tran-Van, F.; Goubard, F.; Teyssié, D.; Chevrot, C. *Eur. Polym. J.* **2008**, *44*, 3864–3870.

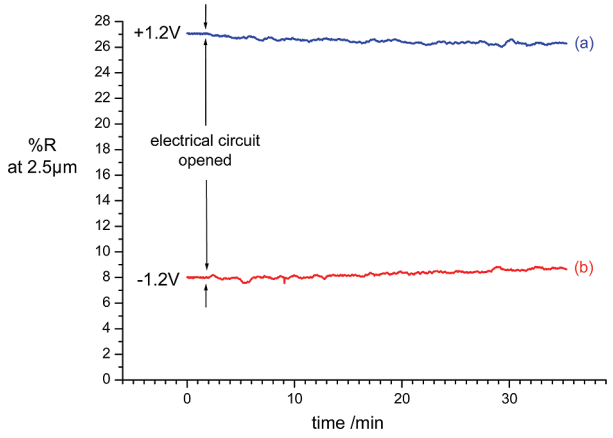

Figure 10. Memory effect of the active surface recorded during 35 min after initial oxidation (curve a) or reduction (curve b) of the active layer. EMITFSI content: 20 wt %.

is producing hydroxyl radical $OH^{\bullet}$ upon thermal activation. These radicals can react on the PEDOT backbone leading to the loss of its electroactivity and hence the loss of reflective properties.

Finally, the memory effect of the device was measured at ambient temperature again for 20 wt % content in EMImTFSI. First, the device was polarized at −1.2 or +1.2 V during 10 min. Then, the evolution of reflectivity at 2.5 μm was monitored as a function of time after suppression of the applied voltage (open circuit). Figure 10 shows the variation of the reflectance $\%R_{2.5\ \mu m}$ in both oxidized and reduced states (curves a and b, respectively). The reflectance loss rate is 0.01 $R\% \cdot min^{-1}$ and 0.03% $R \cdot min^{-1}$, respectively, when measured over a 35 min range, which is remarkable. Indeed, it means that the active layer can maintain optimal conditions (low or high reflectance levels) for a long period with as low as possible an energy consumption.

Conclusions

In this work, flexible EMImTFSI-swollen PEO/PEDOT semi-IPN are proposed as new self-supported electroreflective devices exhibiting significant and tunable reflectance variations in infrared as a function of the applied voltage. Indeed, it is reported for the first time that the semi-IPN material actually is the device, without the need for additional gold, ITO, or other extra layers. The PEDOT formed under the surface of the semi-IPN film acts both as a current collector and an active material in the design of the cell. The relationship between the oxidation state of PEDOT, dielectric properties, and optical properties is established deriving from the CS-AFM image analysis and spectroelectrochemical study. Furthermore, self-supported PEO/PEDOT semi-IPNs can be advantageously used as flexible infrared electroreflective devices since switching from conducting to insulating states of the PEDOT component in the matrix induces a drastic change in the reflecting properties of the device, i.e., the reflectivity contrasts equal to $\Delta\% R = 30\%$ and 37% in IR bands II and III, respectively.

Acknowledgment. We thank DGA (Délégation Générale de l'Armement) for funding support.